Available online at www.sciencedirect.com

ScienceDirect

journal homepage: www.intl.elsevierhealth.com/journals/dema

An *in vitro* study of a novel quaternary ammonium silane endodontic irrigant

U. Daood[a,*,1], *A. Parolia*[a,1], *A. Elkezza*[a], *C.K. Yiu*[b], *P. Abbott*[c], *J.P. Matinlinna*[d], *A.S. Fawzy*[c]

[a] *Clinical Dentistry, Restorative Division, School of Dentistry, International Medical University Kuala Lumpur, 126, Jalan Jalil Perkasa 19, 57000 Bukit Jalil, Wilayah Persekutuan Kuala Lumpur, Malaysia*
[b] *Paediatric Dentistry and Orthodontics, Faculty of Dentistry, The University of Hong Kong, Prince Philip Dental Hospital, 34 Hospital Road, Sai Ying Pun, Hong Kong Special Administrative Region*
[c] *UWA Dental School, University of Western Australia, 17 Monash Avenue, Nedlands, WA 6009, Australia*
[d] *Dental Materials Science, Applied Oral Sciences, Faculty of Dentistry, The University of Hong Kong, 34 Hospital Road, Sai Ying Pun, Hong Kong Special Administrative Region*

ARTICLE INFO

Article history:
Received 2 March 2019
Received in revised form
19 May 2019
Accepted 22 May 2019

Keywords:
Root dentine
Quaternary ammonium silane
Condensation
E. faecalis
Antimicrobial
Raman spectroscopy
Confocal microscopy

ABSTRACT

Objective. To analyze effect of NaOCl + 2% quaternary ammonium silane (QAS)-containing novel irrigant against bacteria impregnated inside the root canal system, and to evaluate its antimicrobial and mechanical potential of dentine substrate.

Methods. Root canal was prepared using stainless steel K-files™ and ProTaper™ and subjected to manual and ultrasonic irrigation using 6% NaOCl + 2% CHX, 6% NaOCl + 2% QAS and saline as control. For confocal-microscopy, Raman spectroscopy and SEM analysis before and after treatment, *Enterococcus faecalis* cultured for 7 days. Raman spectroscopy analysis was done across cut section of gutta percha/sealer-dentine to detect resin infiltration. Indentation of mechanical properties was evaluated using a Berkovich indenter. The contact angle of irrigants and surface free energy were evaluated. Mineralization nodules were detected through Alazarin red after 14 days.

Results. Control biofilms showed dense green colonies. Majority of *E. faecalis* bacteria were present in biofilm fluoresced red in NaOCl + 2% QAS group. There was reduction of 484 cm^{-1} Raman band and its intensity reached lowest with NaOCl + 2% QAS. There was an increase in 1350–1420 cm^{-1} intensity in the NaOCl + 2% CHX groups. Gradual decrease in 1639 cm^{-1} and 1609 cm^{-1} Raman signal ratios were seen in the resin-depth region of 17 μm>, 14.1 μm> and 13.2 μm for NaOCl + 2% QAS, NaOCl + 2% CHX and control groups respectively. All obturated groups showed an intact sealer/dentine interface with a few notable differences. 0.771 and 83.5% creep indentation distance for NaOCl + 2% QAS ultrasonic groups were observed. Highest proportion of polar component was significantly found in the NaOCl + 2% QAS groups which was significantly higher as compared to other groups. Mineralized nodules were increased in NaOCl + 2% QAS.

* *Corresponding author at*: Clinical Dentistry, Restorative Division, Faculty of Dentistry, International Medical University Kuala Lumpur, 126, Jalan Jalil Perkasa 19, 57000 Bukit Jalil, Wilayah Persekutuan Kuala Lumpur, Malaysia.
E-mail address: umerdaood@imu.edu.my (U. Daood).
https://doi.org/10.1016/j.dental.2019.05.020

Significance. Favorable antimicrobial and endodontic profile of the NaOCl + 2% QAS solution might suggest clinical use for it for more predictable reduction of intracanal bacteria.

1. Introduction

Microorganisms breach dental hard tissues via acidic dissolution [1] through cracks in tooth or exposed dentinal tubules and reach pulp space to cause infection [2]. Given that, endodontic failure may occur because of bacterial penetration or persistence within the root canal system as result of poor disinfection procedure [3]. Plentiful rinsing is required to clean and disinfect the root canal system for preparation and completion of endodontic procedure [4]. Current guidelines for root canal treatment [5] advocate the idea for the use of voluminous irrigating solution avoiding its extrusion through the apical foramen. Irrigation is usually carried out using a syringe and a needle, which may not be able to clean and disinfect remote areas of the root canal system [6]. During normal clinical practice many techniques have been adapted by dental practioners. Therefore, many elaborate methods were developed in the past to improve root canal disinfection [7]. Most widely used adjunct method for root canal irrigation is ultrasonic agitation [8].

Most of the attention has been given to the use of chlorhexidine (CHX) when dealing with antimicrobials. CHX is bactericidal in high concentrations and bacteriostatic in low concentrations, primarily against gram-positive bacteria [9]. Chlorhexidine is water-soluble and has reversible electrostatic bonding between protonated amine groups [10] leading to eventual leaching out from bonded interfaces, with loss of antimicrobial and protease inhibitory activities in the presence of calcium due to chelation [11]. When NaOCl is used in conjunction with CHX, the former is left behind inside the canal system, and CHX forms a brown precipitate [12], containing *para*-chloroaniline (PCA) with subsequent discoloration and a possible hindrance in the sealing of the obturating material along with blockage of the lateral canals [13]. Therefore, an intermediate rinse is recommended after each irrigant solution. Some studies suggest that the precipitate contains PCA due to the chemical interaction between CHX and NaOCl [14]. Even so, other studies have suggested that this precipitate did not contain PCA [15]. However, the aim of the present laboratory study was not to investigate the deposits formed. Moreover, there is a clinical need to look for alternative irrigation material and regimen.

Nevertheless, some issues like incomplete elimination of bacteria, and weakening of antibacterial actions have led to exploration of alternative options. It is, therefore, vital to develop a novel irrigant or disinfectant with predictable strong antibacterial effects. That said, such a novel material should exhibit no adverse effect on the subsequently applied resin sealers. Quaternary ammonium compounds represent an effective class of antimicrobial agents [16]. The sol–gel process has been used for the design of silica (SiO_2)-based materials in the context of silica gel formation. The hydrolysis process produces silanol groups (—Si—OH) and the reaction proceeds and is followed by condensation of Si—O—Si bonds with inorganic polymerization [17]. The reactions indicate a typical sequence of condensation products that include monomer, dimers and higher order molecular ring products [18]. The silicon atom center has a direct interaction with the solvents as the condensation occurs near the terminal silanol groups, forming a chain-like structure inside the sol and network like gels [19].

The most common compounds that participate in the silica sol-gel chemical reaction are tetramethoxysilane (TMOS) or tetraethoxysilane (TEOS). Tetraethoxysilane acts as an anchoring unit in the formation of the 3D siloxane network. As hydrolysis and condensation proceed further, the —OH and O—Si-units, attached to a specific silicon atom, are increased [20]. The experimental versions of novel quaternary ammonium silane (SiQAS) disinfectant (K21 molecule) examined in the present study were synthesised by sol–gel reaction. Because methanol is produced during the hydrolysis and condensation reactions of SiQAC the molecule is potentially toxic for intraoral use [21]. Hence, SiQAC has been substituted with 3-(triethoxysilyl)-propyldimethyloctadecyl ammonium chloride (i.e. the ethoxy substituted SiQAC, abbreviated as Et-SiQAC) for coupling with tetraethoxysilane (TEOS) via sol–gel synthesis. This resulted in the generation of ethanol- or acetone-soluble, fully-hydrolysed, partially-condensed QAS (1-octadecanaminium, *N,N'*-[[3,3-*bis*[[[3-(dimethyloctadecylammonio) propyl] dihydroxysilyl]oxy]-1,1,5,5,-tetrahydroxyl-1,5-trisiloxanediyl]di-3,1-propanediyl]-*bis*[*N,N*-dimethyl] chloride (1:4), with the CAS number 1566577-36-3 (codenamed K21). The yellow, partially condensed solid was converted into granular powder in absence of ethanol by pressurized reaction mixture under low pressure. The compound was immediately dissolved in absolute ethanol to produce solutions containing 2 wt%, QAS to be used as the experimental irrigant in the present study. However, it is not known whether a QAS-containing disinfectant has the same inhibitory effects against bacteria when impregnated in radicular dentine and canals.

Accordingly, the objectives of present laboratory study were to investigate the effect of a NaOCl + 2% QAS-containing disinfectant/irrigant system against bacteria impregnated into the root canal system, and to evaluate its antimicrobial potential. Considering the complex endodontic system and the difficulty of penetrating dentinal tubules, with concerns of possible PCA and deposits being formed after use of CHX and NaOCl, there is a potential to exploit the QAS disinfectant as an irrigant for a feasible therapeutic approach against biofilm infection

[1] Equal contribution authors.

within the root canal system. The null hypotheses tested were that NaOCl + 2% QAS cavity irrigants had (i) no antimicrobial effect on *Enterococcus faecalis* species biofilm architecture, (ii) no effect on *E. faecalis* species adhesion on dentine structure, and (iii) no effect on mechanical properties of dentine substrate.

2. Materials and methods

2.1. Manufacture of quaternary ammonium silane powder

The 2% QAS irrigant examined was synthesized by sol-gel reaction between 1 mol of TEOS (M_w 208 g mol^{-1}) and 4 mol of Et-SiQAC (M_w 538 g mol^{-1}) as reported previously Daood et al. [35]. Briefly, 1 mol of TEOS (M_w 208 g mol^{-1}) and 4 mol of 3-(triethoxysilyl)-propyldimethyloctadecyl ammonium chloride (i.e. the ethoxy substituted SiQAC, abbreviated as Et-SiQAC; M_w 538 g mol^{-1}). In a typical synthesis, 2.08 g of TEOS was blended with 29.89 g of 3-(triethoxysilyl)-propyldimethyloctadecyl ammonium chloride (72% of Et-SiQAC dissolved in ethanol) and 5 mL of ethanol (to render the blend more homogeneous). Hydrolysis was initiated by the addition of 10.08 g of 0.02 M HCl-acidified deionized water. The pH was set 1.66, representing 3.5 times the stoichiometric molar concentration of water required, to ensure complete hydrolysis. Completion of the hydrolysis reaction took approximately 3 h and it was indicated by the disappearance of absorbance peaks of the Si—O—C peak at 1078 cm^{-1} and the —OC_2H_5 peak at 1172 cm^{-1} as it was monitored by FTIR. The IR spectrum of the fully hydrolysed reaction was characterised by the presence of silanol groups, water and ethanol. There was presence of Si—O—Si cyclic or open chained species identified as impurities (Fig. 1A). Since ethanol is a by-product of the sol–gel reaction and there is elimination of methanol, QAS was successfully used without further purification [22] in all our studies [23,54,62].

2.2. Canal irrigation

Eighty extracted non-carious human single rooted anterior teeth were obtained from patients (21–29 years old) with their informed consent under a protocol reviewed and approved by Institutional Review Board of International Medical University, JC Committee (IMU 425–2018). All the experiments were carried out in accordance with approved guidelines and regulations. Teeth were stored in 0.02% sodium azide at 4 °C to prevent bacterial growth and were used in less than 1 month after extraction. Teeth were cleaned using periodontal curettes to remove periodontal tissues and stored in saline. A low-speed diamond edge-coated disc (Bredent®, Senden, Germany) mounted on a milling machine (K9 Milling Apparatus-990, Kavo, München, Germany) under water cooling was used to decoronate the tooth 1 mm below the cemento-enamel junction to obtain the root segment. Root canal preparation was performed by a single trained endodontist. Root canals were shaped using stainless steel K-files™ (Dentsply Sirona, Tulsa Dental, USA) using watch wind motion.

For ProTaper™ shaping, rotary instruments (both Dentsply Maillefer, Ballagues, Switzerland) were used up to size X4 and irrigated with 2 mL of 6% NaOCl (Calasept, Upplands Väsby, Sweden) after each use. Smear layer of root canals were removed using 6% NaOCl and 17% EDTA (Pulpdent Corporation, Warwick, UK) for 2 min and canals thoroughly rinsed with sterile saline after each irrigation. These teeth were further subjected to sterilization by autoclave for 20 min at 121 °C. Thereafter, these teeth were randomly assigned in six study groups ($n = 5$) and subjected to one of the following irrigation protocols:

Group A: 6% NaOCl + 2% CHX (Manual irrigation using 30-gauge side vented needle, Endo-EZE, Ultradent).

Group B: 6% NaOCl + 2% CHX (UltraSonic agitation, VDW Ultra, VDW GmbH, Munich, Germany).

Group C: 6% NaOCl + 2% QAS (Manual irrigation using 30-gauge side vented needle, Endo-EZE, Ultradent).

Group D: 6% NaOCl + 2% QAS (UltraSonic agitation, VDW Ultra, VDW GmbH, Munich, Germany).

Group E: Saline (Manual irrigation using 30-gauge side vented needle, Endo-EZE, Ultradent).

Group F: Saline (UltraSonic agitation, VDW GmbH, Munich, Germany).

2.3. Teeth preparation

For confocal microscopy, Raman spectroscopy and SEM analysis before and after treatment, the teeth ($n = 5$ per group) were prepared to a size of 50 K-file which was 1 mm short of the apical foramen using crown down technique. Crowns were sectioned using low-speed diamond edge-coated disc (Bredent®, Senden, Germany) mounted on a milling machine and length standardized to 16 mm from coronal to apex of the root. EDTA was added for 3 min for removal of the smear layer and the teeth were autoclaved at 120 °C for 30 min. *E. faecalis* (ATCC 29212) was cultured in 10 mL BHI broth supplemented with 8% sucrose (pH 7.4) and a minimal amount of xylitol (0–2%) was added at 37 °C for 48 h and later incubated at 37 °C for 24 h. After 4000 rpm centrifugation for 15 min, each of the cell pellets was washed three times with sterile phosphate buffered solution (PBS, 0.01 M, pH 7.2), later re-suspended (O.D reading of 0.11 at 660 nm) in 100 mL of the respective growth medium and adjusted to a concentration of McFarland 3 (10^9 cells/mL) before use.

Five milliliters of BHI broth was mixed with equal weight of bacterial inoculum using sterilized syringes of sufficient volume to fill the root canal during a 7-day period. After 7 days, each tooth, under aseptic conditions, were dried with sterile paper points. After subjecting the specimens to different irrigation protocols (no irrigation protocol for control specimens), two parallel grooves were prepared on external surfaces in the mesio-distal direction of each tooth to facilitate split fracture. Final separation was made using a chisel and a hammer and teeth were then taken for SEM, confocal microscopy and Raman analysis.

2.4. Raman spectroscopy for resin sealer penetration

After irrigation with designated protocols for each study group, the root canals were dried with paper points and speci-

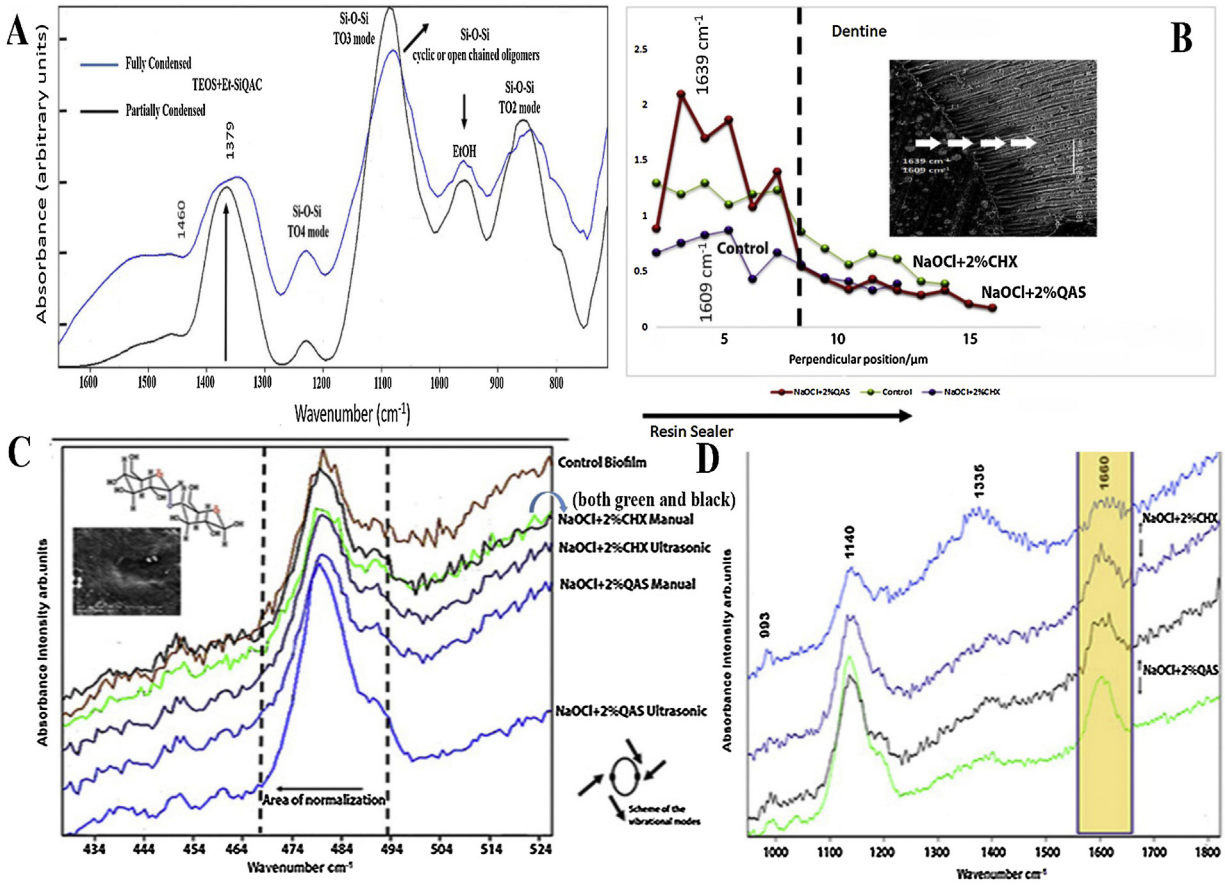

Fig. 1 – (A) Comparison between the partially and fully condensed K21 QAS solution with ethanol as the reference; (B) Representative line map (scans) across sealer interface of different control and after different irrigation protocols specimens. The spectral contribution is recorded at 1639 cm^{-1} and 1609 cm^{-1} obtained ratio intensities representing the penetration of different groups. (C) Raman spectra of *E. faecalis* biofilms on root dentine specimens treated with different irrigation protocols. Spectral differences of control and treated specimens can be seen in the 484 cm^{-1} region after normalization. Biofilm colonies after inoculation and irrigation protocol exposure providing initial comparison with standard signature Raman spectra and change in intensities. (D) Raman spectra of root dentine with treated biofilms cultivation. Yellow region indicates the variation of peaks after treatment at Amide I region with peak based discrimination. (For interpretation of the references to color in this figure legend, the reader is referred to the web version of this article.)

mens ($n = 3$) were then randomly assigned to each study group, based on the irrigation protocol. The materials (RealSeal SE and gutta percha) for obturation were manipulated according to the manufacturer's instructions and canals sealed using single cone obturation technique. Each root section was cut horizontally into approximately 1 mm thick slices to obtain the middle third sections and each section subjected for Raman spectroscopy analysis. The spectra were obtained using a Raman spectrometer equipped with a Leica microscope and lenses (JY LabRam HR 800, Horiba Jobin Yvon, France) with curve-fitting Raman software (Labspec 5). The Raman spectra was obtained using the 785 nm laser source at 50× magnification and a spectral resolution of 1 cm^{-1} and a laser power of 4.94 mW. The laser beam was focused across the cut section of the gutta percha/sealer-dentine interface. Readings were taken from the central regions of the specimen interface starting in the resin region of the specimen (on the left), across the interface and ending onto the dentin side of the specimen (on the right) in 1 μm steps using the *x*–*y*–*z* stage to detect resin infiltration and background-corrected for dark counts with intensity normalization. Origin 8 (Origin Lab Corp, Northampton, MA) was used to calculate sealer penetration. The peak intensity at 1609 cm^{-1} was considered as an internal standard for aromatic C=C and 1639 cm^{-1} which is the aliphatic C=C, is indicative of cured seal.

2.5. *Biofilm preparation and Raman spectroscopy data acquisition*

For Raman spectroscopy measurements, specimens were removed after 7 days from culture plates, and allowed to dry for 15 min at 35 °C. The specimens were transferred to microscopic slides (low fluorescent quartz). Areas of 5 μm chosen randomly across all dried biofilm disc specimens. Raman spectra were recorded using a Raman spectrometer (Nanocat, University of Malaya) equipped with a Leica microscope and lenses (JY LabRam HR 800, Horiba Jobin Yvon, France) with curve-fitting Raman spectroscopy software (Labspec 5). The

spectra were collected at 785 nm wavelength with argon ion 632.8 nm laser at a <500 μW power and a 100× objective (a superior signal/noise ratio). The exposure time was 60 s as the sample (including the biofilm specimens) was translated at 0.5 μm intervals in X and Y directions with 1 s exposure time in the information-rich region between 200 and 3200 cm^{-1}. All spectra were recorded at room temperature and in dark to avoid any peaks (background noise) originating due to ambient light. Raman peaks were centered at 434 cm^{-1} (assigned to stretching vibration of V_2PO_4) [24], 960 cm^{-1} (hydroxyapatite PO_4) [25] for inorganic species, and, 484 cm^{-1} (polysaccharides or carbohydrates) [26], 1655 cm^{-1} (amide I {C=O}) [27], and 1454 cm^{-1} (pyrrolidine rings of proline and hydroxyproline inside collagen) [28] for organic to the peak at 1070 cm^{-1}.

2.6. Confocal analysis

Non-destructive identification of QAS within the root dentinal surface was performed using 0.1 wt% aqueous solution of sodium fluorescein (46960 Bioreagent, Millipore Sigma, Darmstadt, Germany).

After irrigation with NaOCl + 2% QAS the specimens ($n = 3$) were rinsed in 0.1 wt% fluorescein for 24 h. The specimens rinsed with deionised water were examined using confocal laser scanning microscope (CLSM, Leica Fluoview FV 1000, Olympus, Tokyo, Japan), equipped with a 60×/1.4 NA oil immersion lens using 488 nm argon/helium laser beam and 633 nm krypton ion laser illumination, both in the reflection and fluorescence modes. Reflected and fluorescence signals were detected with a photomultiplier tube to a depth of 20 μm and then converted to single-projection images for better visualization and qualitative analysis. Stacks of fluorescent images obtained of the biofilm were examined using bioimageL software (v.2.0. Malmö, Sweden), which provides information on the structure of the biofilm, including green and red-stained bacteria volume on a two dimensional x–y section based on color segmentation algorithms written in MATLAB.

2.7. SEM analysis

For SEM analysis of biofilms, the specimens (preparation described above in Section 2.2) were placed onto the SEM sample holder and imaging was performed at 3500× magnifications at a working distance of 5–8 mm to aid in locating the same area after specimen placement, to be used as markers for accurate co-registration. Next, images were cropped to the same size to enable batch processing in the segmentation step.

As expected, neutralization of QAS irrigant would take place by the buffering action of dentine leading to a condensation of 3D network within and around the dentine tubules. Dentine canals in specimens ($n = 3$) were subjected to NaOCl + 2% CHX or NaOCl + 2% QAS irrigation protocol according to the groups. Two parallel grooves were made onto the external surfaces, in the mesio-distal direction to facilitate a split fracture. Final separation was made using a chisel and a hammer. All specimens were dehydrated in ascending grades of ethanol (33%, 66%, 85%, 95%, 2 × 100%, for 20 min in each) and immediately transferred to the pressure chamber of the critical point drying machine (CPD 30, Leica). The specimens were mounted on aluminium stubs (specimen holders) with double-sided conductive tape, sputter-coated with 30 nm thick layer Au/Pd (120 s) and examined using a SEM (Philips/FEI XL30 FEG SEM) at an accelerated voltage of 10 kV at different magnifications and images evaluated by two examiners.

The interface morphology between root dentine and resin-based sealer were investigated using SEM. From each apical third, two 1 mm slices were cut, polished sequentially to 1200 grit size by silicon carbide papers (Carbimet, Buehler, Lake Bluff, IL, USA) and slices were prepared for resin infiltration into dentine and resin tag formation. The slices were acid etched using 35% phosphoric acid (15 s) and then rinsed using distilled water for 15 s. The specimens were immersed in 5.25% NaOCl solution for 15 min and rinsed under running water for 5 min. Next, all specimens were post fixed using osmium tetroxide (OsO_4), rinsed using PBS solution, dehydrated in ascending ethanol for 20 min. and dried in a critical-point dryer (CPD30 Baltec, Leica, Guyancourt, France). After air-drying, the specimens were mounted on stubs and gold sputtered for 120 s under vacuum and imaged using a Philips/FEI XL30 FEG at an accelerating voltage of 10 kV.

2.8. Nano-indentation testing

A low-speed diamond edge-coated disc (Bredent®, Senden, Germany) mounted on a milling machine (K9 Milling Apparatus-990, Kavo, Germany) under water cooling was used to decoronate the tooth 1 mm below the cemento-enamel junction to obtain the root segment. After following the irrigation protocols, indentation mechanical properties of radicular root canal dentine ($n = 5$) were evaluated using Nanoscope III (Digital Instruments, Santa Barbara, CA) with a Berkovich indenter (Hysitron, Minneapolis, MN, USA). An average of ten measurements were taken 1.5 mm apart at 6 N force, 2 Hz speed and 10 indentations per cycle at the root canal lumen. The indentations were available at the following parameters: the first indentation cyclic (the distance between first and last cycles), the creep indentation distance (a progressive rise during application of force from the first indentation) and increased indentation (the distance between the first and last indentation 'distances'). In addition to this, specimens were carbon coated and a Philips/FEI XL30 FEG unit at an accelerating voltage of 10 kV was used to confirm the appearance and location of indentations.

2.9. Contact angles and surface free energy measurements

After selecting the designated irrigation regimens for root dentine specimens, the teeth were horizontally sectioned 1 mm below the cemento-enamel juncion to obtain 5 mm dentine blocks (DB) for each group. Each dentine block was split into 2 semi-cylindrical halves. Deionized water was used as the reference liquid for contact angle measurements. Each irrigant reference liquid was applied in the form of a drop (2 μL) and profile recorded using contact angle analyzer (Dental Simulation Lab, IMU Laboratory). After analysis, Image J software was used for calculating the contact angle fitting within the con-

tour of the droplet, placed on the dentine surface. The surface free energy was calculated using the equation [29]:

$$\gamma_L(1-\cos\theta) = 2[(\gamma_L^D\gamma_S^D)^{0.5} + (\gamma_L^+\gamma_S^-)^{0.5} + (\gamma_L^+\gamma_S^-)^{0.5}] \quad (1)$$

where, γ, θ are the contact angle and surface tension of reference liquid used. L and S subscripts represent different phases, whereas superscripts D, −, and + represent dispersive and the Lewis bases. All images captured were taken in 5 min after their placement on the dentine surface.

2.10. Alazarin red staining

Mineralization nodules were detected through Alazarin red staining after performing 14 days of induction following application of root canal irrigation systems on root dentine surface ($n = 5$). A 0.5 mm thick dentine disc was prepared from the middle-root dentine of each tooth giving square-shaped root dentine discs. The final disc thickness of approximately 0.4 mm. It was achieved by grinding the outer side with wet 320 grit silicon carbide papers. The NIH 3T3 MF cell line was cultured in Dulbecco's Modified Eagle's Medium (DMEM, Sigma Aldrich, St. Louis, MO, USA) with 1% penicillin/streptomycin (10,000 U/100 μg/mL) and 10% fetal bovine serum (FBS) in a humidified incubator with 5% CO_2 incubator at 37 °C. The cells were cultured to seventh passages and expanded to 4× dilution as the cells reached 85% confluence. After 3 days of incubation, the cells (3×10^4) were seeded on the pulpal side of the root dentine discs (0.28 cm^2) in 24-well plates ($n = 5$) in an incubator with 5% CO_2 and 95% air at 37 °C. Next the discs were transferred back to the same wells to receive the irrigation treatments. The irrigation formulations were applied by placing discs into respective petri dishes containing a 2 mm depth of irrigation formulations for 2 min, followed by blot-drying.

All procedures were performed in a vertical laminar flow hood. After the treatment, the root dentine discs were placed in the CO_2 incubator for additional 24 h. The root dentine discs and cell culture were rinsed twice with PBS, and they were fixed for 1 h using 70% ethanol. After rinsing the specimens thrice using de-ionized water, the specimens were stained using 40 mmol/l Alizarin Red solution (Sigma-Aldrich), adjusted to a pH of 4.0 with ammonium hydroxide for 20 min. Then, the cells were rinsed again with de-ionized water for removal of excess dye. Photographs were taken using a light microscopy (LW 0.52 Nikon Japan, Eclipsee). The cells were counted (0.28 cm^2) in 24-well plates. The cells were then incubated with 10% cetylpyridinium chloride (Sigma-Aldrich) for 15 min to solubilize the nodules. The absorbance of the resulting solution formed for each group was calculated based on the mean value of the control group at 14 days as 100% staining.

2.11. Statistical analysis

All data are presented as mean ± standard deviation and they were analyzed using a statistical package (SigmaStat Version 20, SPSS, Chicago, IL, USA software) assessed for a normal distribution using the Shapiro–Wilk test for normality ($p > 0.05$). One-way analysis of variance followed by the Tukey *post hoc* multiple comparison test, was used to evaluate the antimicrobial effect on the percentages of live and dead bacteria and micro-indentation analysis. All statistical analysis used a 95% confidence limit, so that the p values ≥ 0.05 were not considered statistically significant. The surface free energy was calculated using one-way analysis of variance ($p < 0.05$). One-way ANOVA was also conducted to determine significant differences amongst Alazarin red staining groups (p-value of 0.05).

3. Results

Raman spectroscopy at 1 μm across the interface in all experimental groups is shown in Fig. 1B. A gradual decrease in the 1639 cm^{-1} and 1609 cm^{-1} peak ratios are seen in the region of 17 μm>, 14.1 μm> and 13.2 μm for NaOCl + 2% QAS, NaOCl + 2% CHX and control groups respectively, ending in a plateau assigned by the 1639 cm^{-1}/1609 cm^{-1} ratios. The results indicate a comprehensive penetration of the sealer in NaOCl +2% QAS groups, confirming also a complex interaction between the sealer and specimens. The abrupt decrease in ratio intensities of 1639 cm^{-1}/1609 cm^{-1} in all groups indicate resistance to sealer penetration (Fig. 1B).

From the spectra it can be observed that the bands in this region respond mostly with treatment on the biofilm and typify changes within the absorbance spectrum with intensity changes with different irrigation specimen groups (Fig. 1C). There were obvious variations in spectra with the biofilm changes at 484 cm^{-1} according to the compounds used. The weak bands refer to the glycosidic link or the ring wagging of possible polysaccharides within the biofilm or spectroscopic signature due to linkages of polysaccharides. There was a gradual reduction and striking difference of the 484 cm^{-1} band as the intensity reaches the lowest with NaOCl + 2% QAS groups. This suggests a decrease in the carbohydrate content within the biofilm, again a factor that is more pronounced with the QAS groups. These carbohydrate moieties are more likely complex C—O and C—C stretches coupled with C—H deformations.

The changes within the groups affecting the different biofilms, although highly reproducible, are far more pronounced in Fig. 1D, as tests were performed in triplicates. There is an increase in the underlying intensity in the 1350–1420 cm^{-1} region in the biofilm in the NaOCl + 2% CHX groups suggesting an increase in the carbohydrate content ($p < 0.05$), a factor more pronounced for biofilm backbone. The new band at 993 cm^{-1} supports the argument that we are observing an increase in carbohydrate content in the biofilm ($p < 0.05$). The resolution at 1100 cm^{-1} to 1150 cm^{-1} indicates the peptidoglycan and polysaccharide in this region of the biofilm, which are seen typically high in the NaOCl + 2% CHX groups (Fig. 3).

Representative images of biofilm formed on the specimens are presented in Fig. 2. In the control samples (Fig. 2A), the *E. faecalis* biofilm appears to be in higher quantity covering the dentine surface. The biofilms show densely clustered green colonies (98.71 ± 0.71 live bacteria) with minimal areas of dead bacterial cells. Results of one-way ANOVA verified significantly lower biofilm volume and thickness after the use of irrigation protocols, especially in the case of NaOCl + 2% QAS groups

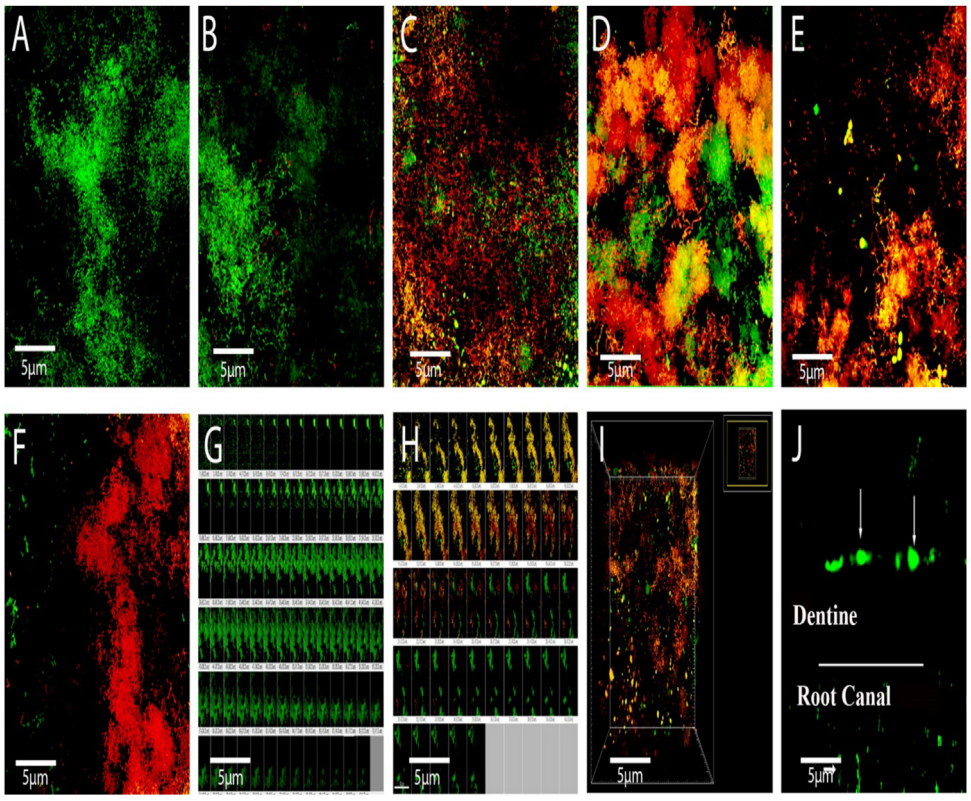

Fig. 2 – CLSM images (A–I) of *E. faecalis* biofilms (100×). Live bacterial cells appeared green; whilst dead cells appeared red. (A and B) Control; (C and D) NaOCl + 2% CHX manual and ultrasonic respectively; (E and F) NaOCl + 2%QAS manual and ultrasonic respectively; (G) control specimens showing 20 μm stack; (H) NaOCl + 2% CHX ultrasonic specimens with 20 μm stack; (I) NaOCl + 2% QAS ultrasonic specimens; (J) CLSM merged image after application of NaOCl + 2% QAS irrigant, with sodium fluorescein staining of 2% QAS. (For interpretation of the references to color in this figure legend, the reader is referred to the web version of this article.)

Table 1 – Bacterial viability in *E. faecalis* species biofilms following different irrigation regimens.

	Dead bacteria			Live bacteria		
	Mean %		SD	Mean %		SD
E. faecalis						
Control	0.23	A	0.88	98.71	a I	0.71
NaOCl + 2% CHX (manual)	69.22	B	5.12	29.78	b II	8.12
NaOCl + 2% CHX (ultrasonic)	84.11	C	6.43	15.69	c III	5.54
NaOCl + 2% QAS (manual)	94.64	D	11.32	5.36	d IV	9.21
NaOCl + 2% QAS (ultrasonic)	97.45	E	3.79	2.33	d IV	6.39

CHX: chlorhexidine, QAS: quaternary ammonium silane.
Values: means ± standard deviation.
Groups identified by different alphabets and numerals were significantly different at $p < 0.05$ in columns and rows respectively.

(manual/ultrasonic). The majority of the *E. faecalis* bacteria present in the biofilm fluoresced red in the NaOCl + 2% QAS group, indicating mostly dead cells (Fig. 2D and E). There were significant reductions of live bacteria within the biofilms that were dependent on the concentration of 2% QAS incorporated into NaOCl irrigations ($p < 0.05$). The highest dead cell count was seen in the biofilm stack within the thickness of NaOCl + 2% QAS groups (Fig. 2H) as compared to control specimens (Fig. 2F). A merged CLSM image of a representative specimen from NaOCl + 2% QAS ultrasonic group is shown in Fig. 2I. The QAS compound was stained using sodium fluorescein as the region corresponded to the root canal edge and inside the root canal (Fig. 2I). The percentages of live and dead bacteria for confocal images using Image J software are given in Table 1.

Scanning electron microscopy images of root dentine after the application of NaOCl + 2% CHX and NaOCl + 2% QAS irrigation regimens are shown in Fig. 3. Now, Fig. 3A shows dentine surface covered with a thick deposit and dentinal tubule orifices are not clearly visible in specimens treated manually with

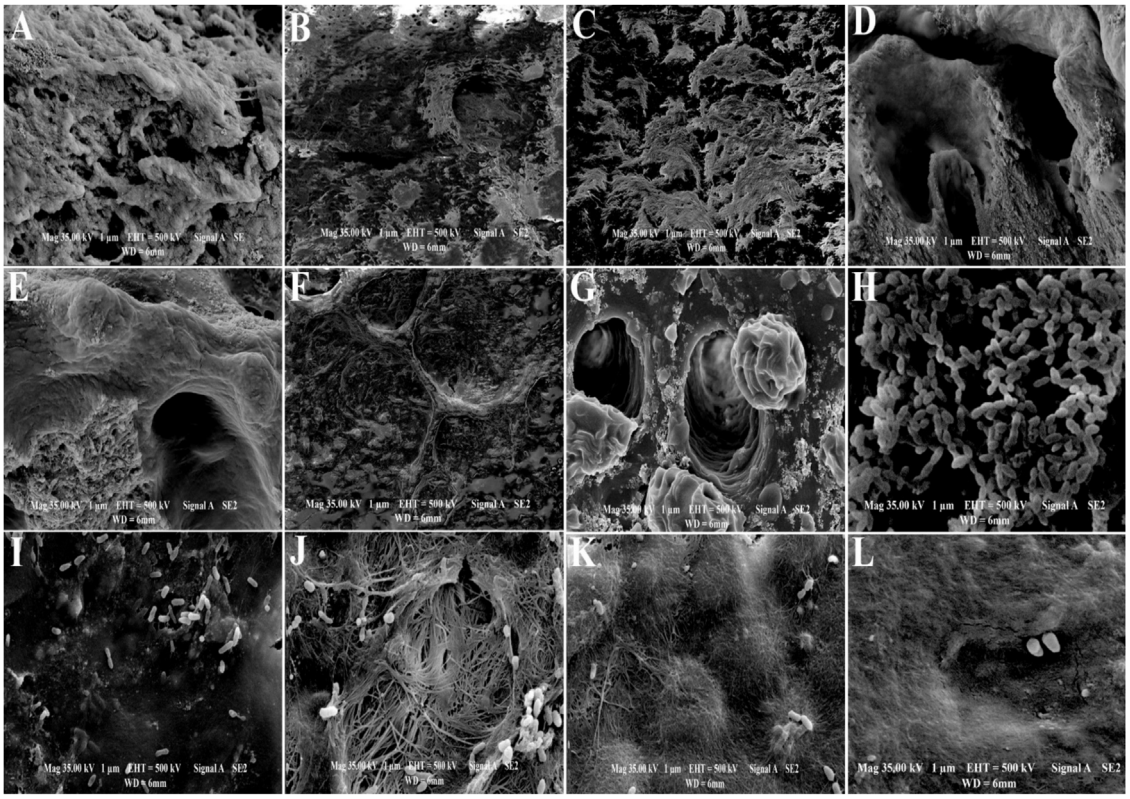

Fig. 3 – Representative SEM images of root dentine following application of (A–C) NaOCl + 2% CHX manual and ultrasonic irrigation protocols. The NaOCl + 2% CHX did not infiltrate well into dentine, but formed huge deposits on the surface. (D) After application of NaOCl + 2% QAS irrigation protocol, the QAS layer was formed on top in the form of a thin crust, in both manual (D) and ultrasonic (E and F) specimens. (G) QAS was seen to be phase separated in the presence of water from dentinal tubules producing spherical structures after ultrasonication. (H) Dense clusters of *E. faecalis* bacterial cells were observed as micro-colonies on the dentine in untreated specimens; (I–J) recolonization of *E. faecalis* on root canal walls is seen in specimens after irrigation with NaOCl + 2% CHX manual (I) and ultrasonic (J) specimens; almost complete eradication of bacterial colonies seen after using NaOCl + 2% QAS protocols in both manual (K) and ultrasonic (L) specimens.

NaOCl + 2% CHX. The groups display multiple and singular deposits covering the sample. Scratches on dentine surface are visible, created by the mechanical preparation, however these scratches show less deposits in the NaOCl + 2% CHX treated specimens with ultrasonic irrigation protocol (Fig. 3B). The degree of dentinal orifice exposure was the lowest for these groups as most of the orifices remained obliterated. The surface is relatively coarse and the deposits are predominantly evenly spread. Fig. 3 shows a crust formation on the dentine surface, in both manual (Fig. 3D) and ultrasonically (Fig. 3E and F) treated specimens with NaOCl + 2% QAS irrigation protocols. There is seen condensation of 2% QAS as spherical bodies on top of the dentinal tubules which is indicative of a phase separation inside the tubules due to the presence of water (Fig. 3G). In the absence of any treatment *E. faecalis* formed monolayer biofilms and micro-colonies are visible and remain the same throughout the specimen with cells chaining and clumping and thereby forming complex biofilms. The most dramatic changes in the biofilm were observed in the NaOCl + 2% QAS specimens following both manual (Fig. 3K) and ultrasonic (Fig. 3L) irrigation protocols, as compared to NaOCl + 2% CHX specimens (Fig. 3I and J). The SEM micrographs demonstrate absence of bacterial colonies in the NaOCl + 2% QAS groups, suggesting that there was increased cell lysis and removal. There were small colony formations in NaOCl + 2% CHX groups due to restructuring of biofilms from monolayers into micro-colonies. While observing specimens from the QAS groups in both manual and ultrasonic irrigation protocols, there was maximum detachment of *E. faecalis* biofilms.

Representative SEM images of the resin sealer/dentine interface of the specimens are shown in Fig. 4. All obturated specimen groups show an intact sealer/dentine interface with a few notable differences between the control, NaOCl + 2% CHX and NaOCl + 2% QAS groups. Well-formed and extensive, long resin tags can be seen forming a continuous intact interface, and also possibly a hybrid layer with the overlying resin sealer, heavily concentrated at the sealer/dentine interface of the NaOCl + 2% QAS manual and ultrasonic specimen groups. The resin tags are penetrating deep into the dentinal tubules appearing as smooth tubular rods (Fig. 6E and F) as compared to the control (Fig. 4A and B). As the irrigation regimen changed, there appears to be a corresponding change in the sealer penetration. However, the NaOCl + 2% CHX specimens (Fig. 4C and D) show an interfacial gap between the resin tags and the sealer, especially in the manual irrigation group (Fig. 4C). No pattern is seen in the manual and ultra-

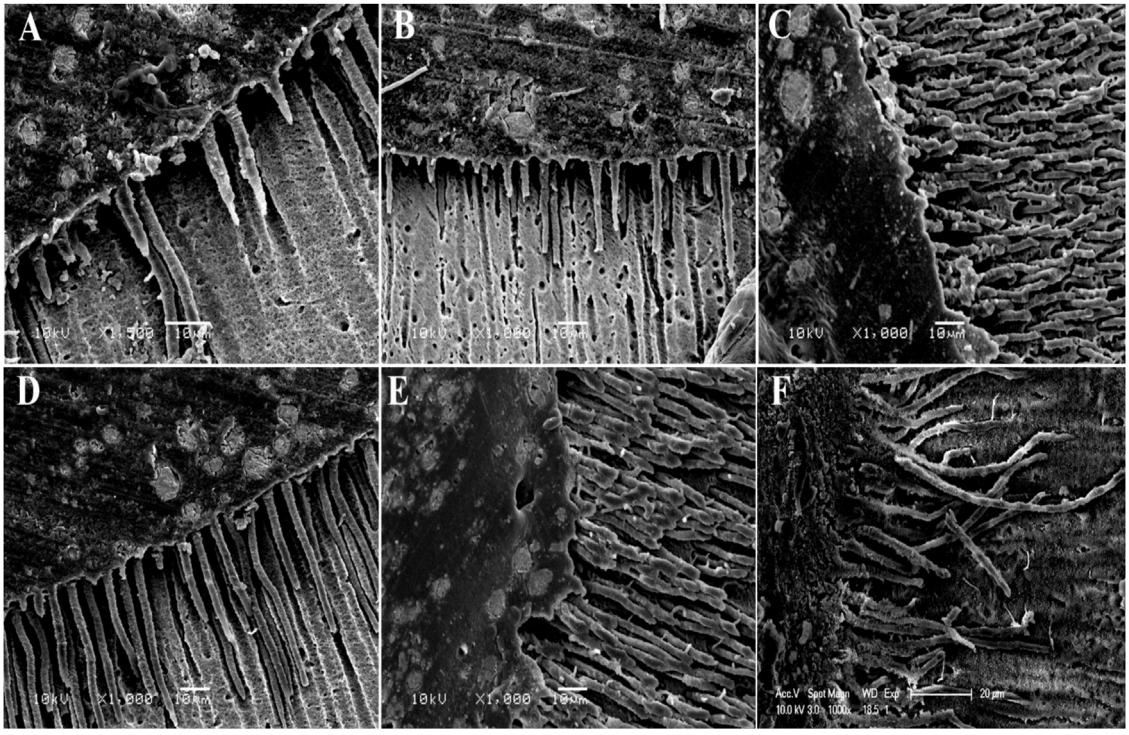

Fig. 4 – Scanning electron microscope images of sealer-dentine interface in (III A and B) manual and ultrasonic control, (III C and D) manual and ultrasonic NaOCl + 2% CHX specimens, and (III E and F) manual and ultrasonic NaOCl + 2% QAS specimens. Note the formation of sealer tags in all specimens.

sonic control specimens, suggesting a correlation between the irrigation and sealer penetration. In the NaOCl + 2% CHX specimens (Fig. 4C and D), the sealers appeared mixed, but non-homogenous, suggesting not all tubules were filled with sealer.

The depth-dependent loading in nano-indentation tests is a good discriminator between the groups and showed that the elastic moduli were constant within a range of 50 nm–150 nm contact depth. The total indentation increase at 95% confidence interval was of 0.771 and 83.5% (95% CI) for creep indentation distance for the NaOCl + 2% QAS ultrasonic groups (Fig. 5). Within this target measurement range, the average elastic modulus for the NaOCl + 2% QAS ultrasonic group (>29.1 ± 3.39 GPa) was significantly higher than compared to the control (<25.3 ± 4.4 GPa) and the NaOCl + 2% CHX (<27.2 ± 2.9) groups ($p < 0.05$) after ultrasonication. The differences between the control and other groups are shown in Table 2. As expected the differences were observed in nano-indentation and elastic moduli indicating measurements of creep indentation and the indentation increase are much higher in the NaOCl + 2% QAS groups, both in the manual and ultrasonic irrigation protocols when compared to all other groups (Fig. 5).

The surface free energy of root canal dentine after application of intracanal irrigant is showed in Fig. 6. Results of one-way ANOVA analysis showed a significant difference among the groups ($p < 0.01$). As compared to control (±109 m/J/m^2 manual; ±140 m/J/m^2 manual), the values for NaOCl + 2% CHX (both groups) (±99 m/J/m^2 manual; ±103 m/J/m^2 manual) were reduced due to a significant difference in the polar components. The highest proportion of polar component was significantly found in the NaOCl + 2% QAS groups which was significantly higher as compared to all other groups (±144 m/J/m^2 manual; ±157 m/J/m^2 manual). For the NaOCl + 2% QAS groups, the estimated γ_S^D values remained different as the γ_S values increased when compared to control.

Deposition of mineralized nodules 14 days after application of irrigation formulations are shown in Fig. 7. Fig. 7A and B is a depiction of 3T3 NIH mouse fibroblastic cells after exposure to the NaOCl + 2% CHX (Fig. 7D) and NaOCl + 2% QAS groups (Fig. 7E) respectively. Mineralized nodules were significantly smaller in the NaOCl + 2% CHX (±2.8) specimens when compared to the NaOCl + 2% QAS (±5.1) specimens and the control (±3.3). In the control specimens, the NIH 3T3 mouse fibroblasts cells revealed positively stained calcium deposits when Alazarin red was used. Lesser staining than in the control groups were seen in the NaOCl + 2% CHX groups. Massive positive dark stainings were seen representing calcium deposits (mineralization) in the NaOCl + 2% QAS groups (Fig. 7E). The use of NaOCl + 2% QAS significantly increased nodule formation after 14 days) ($p < 0.05$).

4. Discussion

The bacterial influence of a more acidogenic environment and aciduric microbiota is a direct consequence of frequent and prolonged acidification, changing the ecological balance in the tooth substrate [30]. In the approach to reduce bacterial acidification mentioned, most attention is paid to reduc-

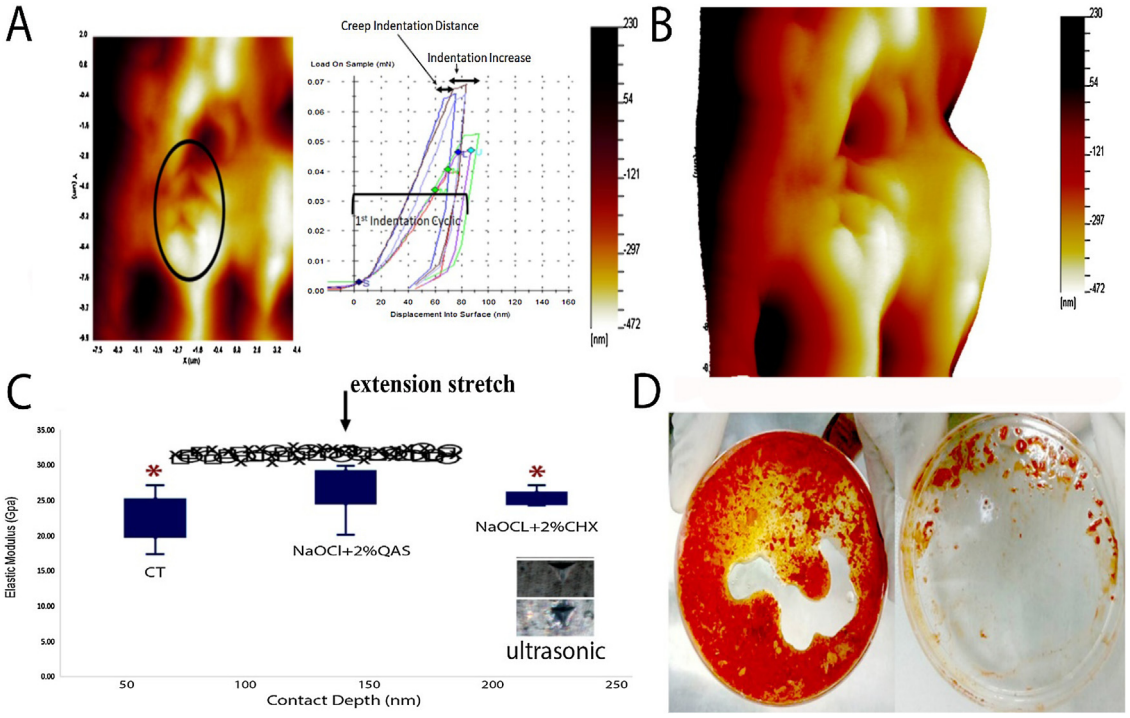

Fig. 5 – Micro indentation distance increase, first indentation cycle and creep indentation parameters measured in the first cycle for (A) manual and (B) ultrasonic NaOCl + 2% QAS irrigation specimens. (C) Indentation load function after depth profiling of elastic modulus (extension stretch identified by arrow) for ultrasonic groups showing statistical similarity for control and NaOCl + 2% CHX groups (*). (D) A representative photograph of deposits/precipitates formed after consequent use of NaOCl and chlorhexidine on culture plates. Note the colour change and deposits in the mixed liquids ranging from dark reddish brown to light orange as well as formation of precipitate in varying amounts. (For interpretation of the references to color in this figure legend, the reader is referred to the web version of this article.)

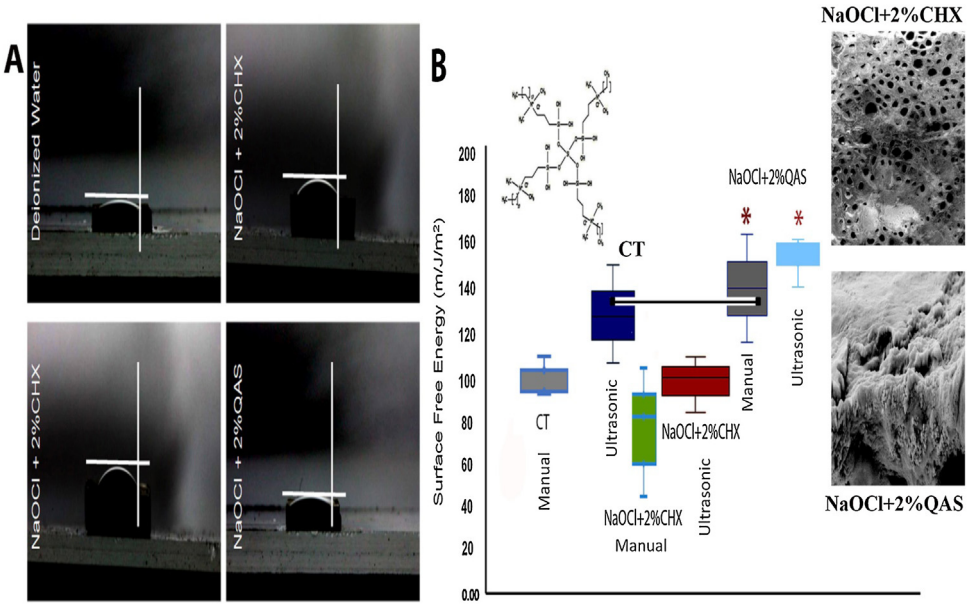

Fig. 6 – Contact angle and (B) surface free energy of root canal dentine with different irrigation regimens. Surface free energy is represented as dispersive and shows significantly higher values for NaOCl + 2% QAS, both manual and ultrasonic specimens. Inset SEM surfaces of root dentine treated with manual NaOCl + 2% CHX and NaOCl + 2%QAS. Both images show presence of deposits and siloxane layer on root dentine surfaces respectively.

Table 2 – Mechanical property analysis of root dentine after different irrigation protocols.

	Nano-indentation			Elastic modulus		
	Creep indentation (μm) (N)		Indentation increase	Values		SD
Control	71.1%	A	0.09	25.3	a I	4.4
NaOCl + 2% CHX (manual)	72.3%	A	0.31	24.6	a I	5.5
NaOCl + 2% CHX (ulrtasonic)	70.1%	A	0.44	27.2	a I	2.9
NaOCl + 2% QAS (manual)	75.9%	B	0.67	27.9	a	7.1
NaOCl + 2% QAS (ultrasonic)	83.5%	C	0.77	29.1	b I	3.4

CHX: chlorhexidine, QAS: quaternary ammonium silane. Values: means ± standard deviation.
Groups identified by different alphabets and numerals were significantly different at $p < 0.05$ in rows and columns respectively.

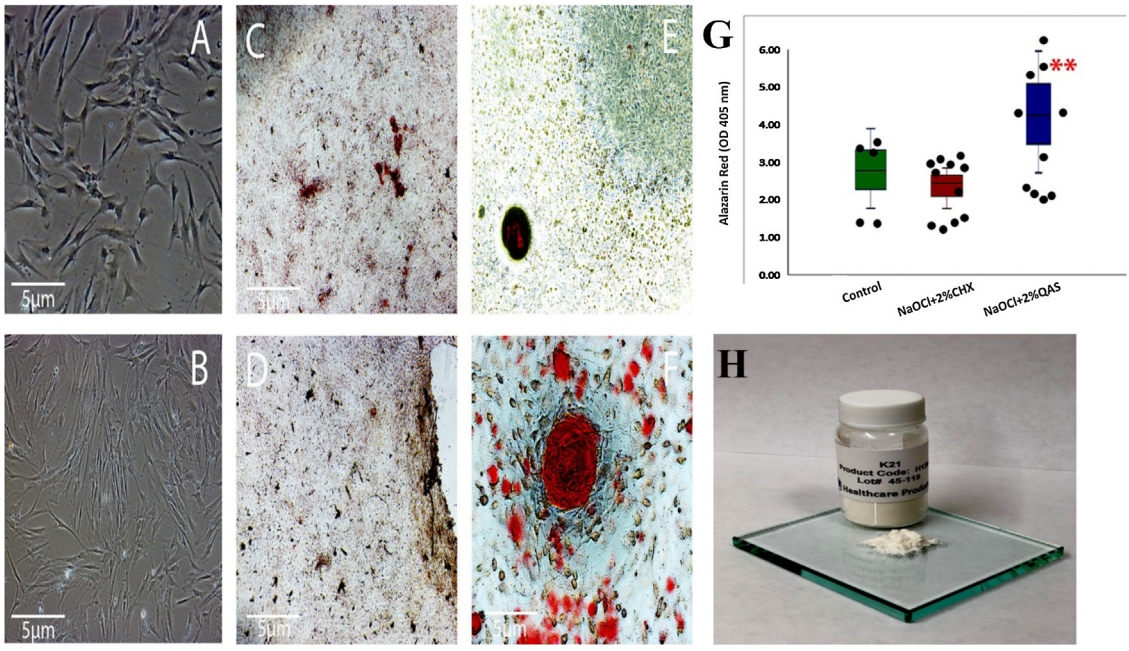

Fig. 7 – 3T3 NIH mouse fibroblastic cells exposed to (A) NaOCl + 2% CHX and (B) NaOCl + 2% QAS irrigants. (C) Light micrographs of minor mineralized nodule 14 days (C) after application of saline on 0.4-mm-thick dentine disc control specimens. (D) NaOCl + 2% CHX specimens barely revealed calcium deposits and did not positively with Alizarin Red S after 14 days; (E and F) Positive dark staining shows presence of calcium deposits i.e. mineralization in 3T3 NIH mouse fibroblasts exposed to NaOCl + 2% QAS. Positive dark red staining shows presence of calcium deposits i.e. mineralization in 2% QAS group after 14 days. (G) Quantification of mineralization differentiation potential in 3T3 NIH mouse fibroblasts using Alazarin Red. Each data point represents a specimen (*$p < 0.05$, not significant. All data represented as mean ± standard deviation). (H) Development of K21 2% QAS powder (*fiteBac Technology USA*) for lipopolysaccharide studies in bacterial membranes.

tion of acid and biofilm formations [31]. Proteolytic anaerobic organisms dominate untreated necrotic root canals while less diverse community dominate the treated ones that can persist for longer periods of time under harsh conditions [32]. Microbial cultures have shown that *E. faecalis* plays a very important role in reinfections of root canals with prevalence up to 24%–77%, and can also survive in severe conditions [33]. One goal of endodontic treatment is to obtain a bacteria free root canal system via irrigation, because it is considered the best method for removal of pulp tissue remnants and dentine debris during instrumentation [34]. Sodium hypochlorite is unable to remove the smear layer and inorganic components during canal instrumentation [35]. The most common methods encompass the use of NaOCl and CHX gluconate as an adjunct in root canal irrigation to improve microbicidal properties [36]. However, if NaOCl is present inside the canal, CHX can form precipitates with surface discoloration, some of which are insoluble in water [37], and a negative effect is formed on the sealing ability of obturating material [38]. That said, an intermediate rinse should be used after each irrigating solution followed by drying the canals to prevent further reactions among the chemical components [39]. Chlorhexidine preparations also delay the time for recontamination of coronally sealed canals. However, the time taken for microorganisms into the root canal was more with CHX solutions as compared to other disinfectant material (calcium hydroxide) [40]. In order to verify our idea for a new root canal irrigant, we used a novel quaternary ammonium silane solution as a disinfectant to research its biological and mechanical impact

on the root dentine surface, because the precipitates formed maybe more cytotoxic than NaOCl and CHX alone [41].

Indeed, organosilane quaternary ammonium salts are a new class of antimicrobials, with reactive silanol groups as a result of generation of hydrolysis OF QAS that are covalently bonded to substrates via Si—O linkages engaging microbiocidal functions [42]. 3-(Trimethoxysilyl) propyldimethyloctadecyl ammonium chloride (SiQAC) has been widely used for antimicrobial coatings of medical devices. It penetrates bacterial cell membranes causing cell death of bacteria as they come in contact. SiQAC salts do not end with polymerizable end functional groups [43]. In general, the positively charged quaternary amine charged (N^+) compounds cause bacterial lysis due to their interaction with the negatively charged bacterial membranes. With the use of SiQAC along an anchoring tetraalkoxysilane and other organofunctional trialkoxysilanes [44], it can produce different antibacterial activities, which remain independent of the loss of surface layer [45]. By altering the pH value of the system, hydrolysis and condensation reactions of QAS can be differentially controlled [46].

To evaluate the antibacterial effects of QAS irrigation protocol, confocal microscopy analysis was done which shows that the QAS irrigation protocol has a significant antimicrobial effect against *E. faecalis* biofilms. Most importantly, endodontic disease is considered as a biofilm-induced infection, as bacteria survive in an adaptive mechanism persisting the endodontic infection [47]. Given this, the incorporation of 2% QAS in the irrigation protocol has potential to render antibacterial properties without a discernable decrease after a prolonged period of time. The QAS compound kills bacteria on contact [48] using TEOS as an anchoring unit and having organic functional groups which are covalently bound and detectable in specimens that showed completely dead bacterial cells (94.64 ± 11.32 and 97.45 ± 3.79 for ultrasonic). This is why the first null hypothesis can be rejected. The CLSM analysis revealed green and red fluorescence intensities within the different biofilms. Most of the bacteria present in the biofilm fluoresced green colour in the control group, indicating that the bacteria were mostly alive in the control. The majority of the bacteria present in the biofilms fluoresced red colour in the QAS groups. This refers to immobilization of the SiQAC molecules that are providing greater antimicrobial activity. Because of the silanol groups, QAS can be covalently bonded via O—Si—O linkages to exert non-migrating microbiocidal functions. The protective antimicrobial film formed results in circumventing or slowing down biofilm formation.

Raman spectroscopy is a widely used powerful tool for identification of bacterial components within the biofilm mass at molecular level [49]. Now, another interesting observation for biofilm in Fig. 1C is the apparent shift of 484 cm^{-1} which is usually assigned to polysaccharides or carbohydrates [50] and has multi-dimensional information on special cellular components and their presence. Even so, the use of different protocols marked a difference in intensities and deviations in structural elements as the control specimens showed intensive signals at 484 cm^{-1}. Moreover, the Raman signals assigned to these polysaccharides were also detected in other samples treated with different irrigation protocols. Based on this compatibility, NaOCl + 2% QAS (manual and ultrasonic) showed the least amount of intensity (Fig. 1C), followed by NaOCl+2%CHX ultrasonic and manual, respectively. These Raman signatures of carbohydrates appeared at lower intensities in QAS specimens hypothesizing that more bacterial colonies are being affected, and endorsing the rejection of null hypothesis. There was also a substantial difference in intensity ratio of Raman bands at 484 cm^{-1} and 1130 cm^{-1} with some shifts (data not shown). The set of bands showed to be highly sensitive and specific for biochemical changes.

There was appearance of new bands near at 993 cm^{-1} and 1335 cm^{-1} in the control specimens (Fig. 1D) strengthening the observation for the increase in carbohydrate content as part of the biofilm matrix [51]. However, the intense bands were dull and of lower intensity in the experimental groups, giving a precise description consistent with the absence of additional, albeit unidentified, carbohydrates. Another interesting observation is the apparent change in the amide I (C=O stretch) band, the β-sheet secondary structure that involves amide and carbonyl functional groups, producing spectral changes. It was not possible to avoid such conformational changes due to the native structure within the biofilm, where the intensity of amide I is low in QAS groups, a frequency distinguishable from the substrate. The lowest amide I values are usually measured at the interior of cell nucleus where more nucleic acids are found [52]. In addition, from the results of the study, the NaOCl + 2% QAS groups showed higher amounts of sealer penetration (Fig. 1B) compared to other groups ($p < 0.05$). Hence, including 2% QAS within the irrigation protocol may provide a long-term antibacterial solution. The unique addition of 2% QAS with a NaOCl irrigant could be considered pivotal and an advisable approach for the attainment of maximum antibacterial and avoid reinfections. This laboratory study also indicates the valid use of Raman spectroscopy, allowing detailed spectral analysis for resin penetration of the sealer.

Analysis of the dentine surface and biofilm formed on dentine substrate had been performed using SEM. The contrasting results in SEM between the CHX and QAS groups might be attributed to the nature of two different solutions used for the irrigation protocol (Fig. 3). The thick deposits with complete coverage of the dentinal tubule orifices are clearly visible in specimens treated both manually and ultrasonically with NaOCl + 2% CHX specimens (Fig. 3B and C). Chlorhexidine can react with remaining NaOCl inside the root canal forming small precipitate clusters, which could be *para*-chloroaniline deposits (Fig. 3A–C). However, the purpose of the present laboratory study was not to study the nature of the deposits *per se*. The impact of an endodontic irrigating solution producing such deposits was clearly visible in the SEM analysis of resin tags formed. The current investigation compared the quality, density and length of resin tags formed in each group (Fig. 4). The type of irrigation protocol performed and the morphology of resin tags formed were directly related. The length of resin tags increased in the QAS groups (Fig. 4E and F) despite the 2% QAS groups forming a crust type deposition on the surface of dentine. The presence of bridged organosiloxane groups in the molecular backbone of QAS, which has affinity for the resinous adhesive [53], might have resulted in better penetration. Without the use of resin sealer, QAS did not infiltrate well inside the dentine (Fig. 4C and D). Moreover, the said crust produced by 2% QAS was completely dissolved and subsequently could no longer be identified inside the resin matrix. Conden-

sation of QAS was observed on the dentine surface indicating a phase separation in the presence of water coming from the dentinal tubules (Fig. 3G). With QAS groups, there might have been an increase in surface hydrophobicity by changing the surface free energy of the dentine substrate [54], resulting in better wettability and enhanced infiltration of resin sealer. These organofunctional silanes also act as water scavengers reacting with wholesome water molecules hydrolysing the alkoxy groups present within the silanes converting them into alcohol (in this case: ethanol) molecules [55]. In addition, the formation of hydrophobic layer due to the presence of QAS leads to more durable hybrid layer formation with reduction of water leading to facilitation of infiltration of adhesives (Raman spectroscopy data not shown).

SEM results suggested that NaOCl with 2% QAS was the most effective method for removing *E. faecalis* biofilm in the root canal system, in both manual and ultrasonic way, when compared to other irrigation techniques. This said method debrided and decontaminated the root surfaces both mechanically and chemically. This could be attributed to the known bactericidal effects of NaOCl and synergistic effects of 2% QAS (Fig. 3K and L). That said, the second null hypothesis can be rejected. The possible reasons for the differences in the efficacy of different irrigation protocols could be the result of advanced synergistic effects of QAS. Previous study has reported important information on the antimicrobial effects of 2%QAS on biofilms indeed [56]. One of the major etiologies of endodontic failure is the persistence of bacterial biofilm even after endodontic therapy [57]. Many methods have been examined including machine-assisted irrigation [58] as *E. faecalis* is a well-studied micro-organism in the endodontic literature because of its virulence [59]. The use of a tetrafunctional organosilane as the anchoring unit for the antimicrobial trialkoxysilane molecules enables a three-dimensional network to be formed once condensation is brought to completion within the dentinal substrate [60].

Our surface free energy results (Fig. 6) did not contrast the existing SEM and confocal results. Even so, there was an increased surface energy in the NaOCl + 2% QAS groups, which may be due to the increased surface roughness due to the presence of QAS surface crust. The results for the flow of irrigants are in concordance with other current data demonstrating that NaOCl + 2% QAS based irrigants exhibited higher flow values than the other study groups. The explanation might be primarily due to the complex interactions between the non-polar and polar components of the root canal and the irrigants dispensed on it. As for the model for calculating surface free energy, the droplet volume and substrate type were equal, and this is why we believe that the difference in the irrigation content may have caused these said discrepancies. The ethanol inclusion the 2% QAS may have increased the surface free energy is suggesting that this irrigation protocol may be an attractive method for endodontic therapy. Once there is the formation of a smear layer on the dentine surface, its characteristics can also determine the level of surface free energy as it is increased with the increase in surface roughness due to changes in the $\gamma_S{}^h$ values, reflecting increase surface density on dentine surface [61].

From a practicing endodontist's point of view, the current results strongly support the use and introduction of this irrigation protocol as an alternative. In addition, the obtained contact angles along with surface free energy studies confirm higher wettability to the long-term success of root canal treatment. On the other hand, the use of EDTA is known to soften the dentine and affect the mechanical properties. The use of quaternary ammonium silanes, despite exhibiting temporal hydrolytic stability after condensation, bring some stability with their molecular siloxane bridges (Table 2). Now, this is rejecting the third null hypothesis that QAS has no effect on mechanical properties of dentine substrate. Ongoing work is being performed to study in depth effects on biofilm at the exopolysaccharide backbone.

Even so, the exudation of dentinal fluid along with cytoplasmic elongations within dentinal tubules may have reduced the inward transdentinal diffusion of QAS agents towards the dental pulp. However, this assumption should be verified in vivo before a final conclusion can be drawn. No detrimental effect on mineralized nodule productions was observed in the NaOCl + 2% QAS groups after 14 days (Fig. 5). The normal deposition of mineralized nodules in NaOCl + 2% QAS formulations indicates that the dentine pulp reparative processes, which are essential tertiary dentine formation, were minimally affected following NaOCl + 2% QAS application, rendering it a safe irrigant for use.

The 2% QAS irrigation formulation did not show cytotoxic effects on 3T3 NIH mouse fibroblast cells (Fig. 7). The predominance of the anti-inflammatory phenotype after its application may stimulate healing and tissue repair [62]. It is noteworthy that the newly developed antibacterial quaternary ammonium silane has also been proven to increase the resistance of dentine collagen to degradation and is promising option for use as a protease inhibitor [33] to improve durability of resin-dentin bonds. Moreover, the favorable antimicrobial and endodontic profile of the NaOCl + 2% QAS could be ascribed to its use as a potential irrigation concept for more predictable reduction of intracanal bacteria and enhancing the versatility of the material and its potential use in dentistry. Future work is underway in the development of a 2% QAS powder formulation to investigate the detailed effects of QAS on undifferentiated stem cells and bacterial lipopolysaccharide membranes looking at its important role in regenerative endodontics.

5. Conclusion

Within the limits of the present study, it may that the newly developed quaternary ammonium silane (2% QAS) increases its bacterial efficacy when used in conjunction with NaOCl as an irrigant impregnated inside a root canal. Considering the complex endodontic system and the difficulty of penetrating dentinal tubules, there is a potential to exploit the QAS disinfectant as an irrigant for a feasible therapeutic approach against biofilm infection within the root canal system.

Acknowledgements

This work was supported in part by the grant IMU 425/2018, School of Dentistry, International Medical University. The authors thank the labs at Nanocat University of Malaya, School

of Dentistry of the International Medical University Kuala Lumpur, the Faculty of Dentistry of at University of Hong Kong for the research experiments and analysis.

REFERENCES

[1] Hojo S, Takahashi N, Yamada T. Acid profile in carious dentin. J Dent Res 1991;70:182–6.
[2] Nagaoka S, Miyazaki Y, Liu HJ, Iwamoto Y, Kitano M, Kawagoe M. Bacterial invasion into dentinal tubules of human vital and non-vital teeth. J Endod 1995;21:70–3.
[3] Siqueira Jr JF. Aetiology of root canal treatment failure: why well-treated teeth can fail. Int Endod J 2001;34:1–10.
[4] Willershausen I, Wolf TG, Schmidtmann I. Survey of root canal irrigating solutions used in dental practices within Germany. Int Endod J 2015;48:654–60.
[5] American Association of Endodontics. Guide to clinical endodontics. 6th ed; 2013. Available at: www.nxtbook.com/nxtbooks/aae/guidetoclinicalendodontics6/. [Accessed 10 October 2017].
[6] Boutsioukis C, van der Sluis LW. Syringe irrigation: blending endodontics and fluid dynamics. In: Basrani B, editor. Endodontic irrigation: chemical disinfection of the root canal system. New York: Springer; 2015. p. 45–64.
[7] Haapasalo M, Shen Y, Qian W, Gao Y. Irrigation in endodontics. Dent Clin North Am 2010;54:299–303.
[8] Dutner J, Mines P, Anderson A. Irrigation trends among American Association of Endodontists members: a web-based survey. J Endod 2012;38:37–40.
[9] Rosenthal S, Spangberg L, Safavi K. Chlorhexidine substantivity in root canal dentin. Oral Surg Oral Med Oral Pathol Oral Radiol Endod 2004;98:488–92.
[10] Breschi L, Mazzoni A, Nato F. Chlorhexidine stabilizes the adhesive interface: a 2-year in vitro study. Dent Mater 2010;26:320–5.
[11] Gendron R, Grenier D, Sorsa T, Mayrand D. Inhibition of the activities of matrix metalloproteinases 2, 8, and 9 by chlorhexidine. Clin Diagn Lab Immunol 1999;6:437–9.
[12] Zehnder M. Root canal irrigants. J Endod 2006;32:389–98.
[13] Gupta H, Kandaswamy D, Manchanda SK, Shourie S. Evaluation of the sealing ability of two sealers after using chlorhexidine as a final irrigant: an in vitro study. J Conserv Dent 2013;16:75–8.
[14] Basrani BR, Manek S, Mathers D. Determination of 4-chloroaniline and its derivatives formed in the interaction of sodium hypochlorite and chlorhexidine by using gas chromatography. J Endod 2010;36:312–4.
[15] Thomas JE, Sem DS. An in vitro spectroscopic analysis to determine whether parachloroaniline is produced from mixing sodium hypochlorite and chlorhexidine. J Endod 2010;36:315–7.
[16] Makvandi P, Jamaledin R, Jabbari M, Nikfarjam N, Borzacchiello. Antibacterial quaternary ammonium compounds in dental materials: a systematic review. Dent Mater 2018;6:851–67.
[17] Turova NY, Turevskaya EP, Kessler VG, Yanovskaya MI. The chemistry of metal alkoxides. Norwell: Kluwer Academic Press; 2002.
[18] Danks AE, Hall SR, Schnepp Z. The evolution of 'sol–gel' chemistry as a technique for materials synthesis. Mater Horiz 2016;3:91–5.
[19] Levy David, Zayat Marcos, editors. The sol–gel handbook: synthesis, characterization, and applications. 1st ed. Wiley-VCH Verlag GmbH & Co. KGaA; 2015. Published 2015 by Wiley-VCH Verlag GmbH & Co. KGaA.
[20] Hoffmann F, Fröba M. Vitalising porous inorganic silica networks with organic functions—PMOs and related hybrid materials. Chem Soc Rev 2011;40:608–20.
[21] Bindler F, Voges R, Laugel P. The problem of methanol concentration admissible in distilled fruit spirits. Food Addit Contam 1988;5:343–51.
[22] Daood U, Yiu CKY, Burrow MF, Niu LN, Tay FR. Effect of a novel quaternary ammonium silane on dentin protease activities. J Dent 2017;58:19–27.
[23] Daood U, Yiu CKY, Burrow MF. Effect of a novel quaternary ammonium silane cavity disinfectant on cariogenic biofilm formation. Clin Oral Invest 2019, http://dx.doi.org/10.1007/s00784-019-02928-7.
[24] Soares LE, do Espirito Santo AM, Junior AB, Zanin FA, da Silva Carvalho C, de Oliveira R, et al. Effects of Er:YAG laser irradiation and manipulation treatments on dentin components, part 1: Fourier transform-Raman study. J Biomed Opt 2009;14:1–7.
[25] Alebrahim MA, Krafft C, Popp J. Raman imaging to study structural and chemical features of the dentin enamel junction. Mater Sci Eng 2015;92:1–9.
[26] Schuster KC, Reese I, Urlaub E, Gapes JR, Lendl B. Multidimensional information on the chemical composition of single bacterial cells by confocal Raman microspectroscopy. Anal Chem 2000;72:5529–34.
[27] Ramakrishnaiah R, Rehman G, Basavarajappa S, Al Kkhuraif AA, Durgesh BH, Khan AS, et al. Applications of Raman spectroscopy in dentistry: analysis of tooth structure. Appl Spectrosc Rev 2015;50:332–50.
[28] Silva Júnior ZS, Botta SB, Ana PA, França CM, Fernandes KP, Ferrari RA, et al. Effect of papain-based gel on type I collagen — spectroscopy applied for microstructural analysis. Sci Rep 2015;5:11448.
[29] Koehne T, Marshall RP, Jeschke A, Kahl-Nieke B, Schinke T, Amling M. Osteopetrosis, osteopetrorickets and hypophosphatemic rickets differentially affect dentin and enamel mineralization. Bone 2013;53:25–33.
[30] Nobuhiro T, Bente N. Ecological hypothesis of dentin and root caries. Caries Res 2016;50:422–31.
[31] Li Y, Tanner A. Effect of antimicrobial interventions on the oral microbiota associated with early childhood caries. Pediatr Dent 2015;37:226–44.
[32] Figdor D, Sundqvist G. A big role for the very small — understanding the endodontic microbial flora. Aust Dent J 2007;52(1Suppl):S38–51.
[33] Stuart CH, Schwartz SA, Beeson TJ, Owatz CB. *Enterococcus faecalis*: its role in root canal treatment failure and current concepts in retreatment. J Endod 2006;2:93–8.
[34] Haapasalo M, Shen Y, Wang Z, Gao Y. Irrigation in endodontics. Braz Dent J 2014;21:299–303.
[35] Teixeira CS, Felippe MCS, Felippe WT. The effect of application time of EDTA and NaOCl on intracanal smear layer removal: an SEM analysis. Int Endod J 2005;38:285–90.
[36] Marco S, Rullo R, Albino A. The thioredoxin system in the dental caries pathogen *Streptococcus mutans* and the food-industry bacterium *Streptococcus thermophilus*. Biochimie 2013;95:2145–56.
[37] Vivacqua-Gomes N, Ferraz CC, Gomes BP, Zaia AA, Teixeira FB, Souza-Filho FJ. Influence of irrigants on the coronal microleakage of laterally condensed gutta-percha root fillings. Int Endod J 2002;35:791–5.
[38] Zehnder M. Root canal irrigants. J Endod 2006;32:389–98.
[39] Vouzara T, Koulaouzidou E, Ziouti F, Economides N. Combined and independent cytotoxicity of sodium hypochlorite, ethylenediaminetetraacetic acid and chlorhexidine. Int Endod J 2016;49:764–73.

[40] Gomes BP, Sato E, Ferraz CC, Teixeira FB, Zaia AA, Souza-Filho FJ. Evaluation of time required for recontamination of coronally sealed canals medicated with calcium hydroxide and chlorhexidine. Int Endod J 2003;36:604–9.
[41] Cintra LT, Watanabe S, Samuel RO, et al. The use of NaOCl in combination with CHX produces cytotoxic product. Clin Oral Investig 2014;18:935–40.
[42] Zhang W, Luo XJ, Niu LN, Liu SY, Zhu WC, Epasinghe J, et al. One-pot synthesis of antibacterial monomers with dual biocidal modes. J Dent 2014;42:1078–95.
[43] Ahlström B, Thompson RA, Edebo L. The effect of hydrocarbon chain length, pH, and temperature on the binding and bactericidal effect of amphiphilic betaine esters on *Salmonella typhimurium*. APMIS 1999;107:318–24.
[44] Matinlinna JP, Lung CYK, Tsoi JKH. Silane adhesion mechanism in dental applications and surface treatments: a review. Dent Mater 2018;34:13–28.
[45] Gong SQ, Niu LN, Kemp LK, Yiu CK, Ryou H, Qi YP, et al. Quaternary ammonium silane-functionalized, methacrylate resin composition with antimicrobial activities and self-repair potential. Acta Biomater 2012;8:3270–82.
[46] Salon MCB, Bayle PA, Abdelmouleh M, Boufi S, Belgacem MN. Kinetics of hydrolysis and self-condensation reactions of silanes by NMR spectroscopy. Colloid Surf A 2008;312:83–91.
[47] Al-Ahmad A, Ameen H, Pelz K, et al. Antibiotic resistance and capacity for biofilm formation of different bacteria isolated from endodontic infections associated with root-filled teeth. J Endod 2014;40:223–30.
[48] Tiller JC, Liao CJ, Lewis K, et al. Designing surfaces that kill bacteria on contact. Proc Natl Acad Sci U S A 2001;98:5981–5.
[49] Efrima S, Zeiri L. Understanding SERS of bacteria. J Raman Spectrosc 2008;40:277–88.
[50] Schuster KC, Reese I, Urlaub E, Gapes JR, Lendl B. Multidimensional information on the chemical composition of single bacterial cells by confocal Raman microspectroscopy. Anal Chem 2000;72:5529–34.
[51] Carey Paul R, Gibson Blake R, Gibson Jordan F, Greenberg Michael E, Heidari-Torkabadi Hossein, Pusztai-Carey Marianne, et al. Defining molecular details of the chemistry of biofilm formation by Raman microspectroscopy. Bichemistry 2017;56(17):2247–50, http://dx.doi.org/10.1021/acs.biochem.7b00116.
[52] Baldassarre L, Giliberti V, Rosa A, Ortolani M, Bonamore A, Baiocco P, et al. Mapping the amide I absorption in single bacteria and mammalian cells with resonant infrared nanospectroscopy. Nanotechnology 2016;27:075101.
[53] Lung CYK, Matinlinna JP. Resin bonding to silicatized zirconia with two and cross-linking silane, part I: experimental. Silicon 2010;2:153–61.
[54] Daood D, Yiu CKY, Burrow MF, Niu LN, Tay FR. Effect of a novel quaternary ammonium silane cavity disinfectant on durability of resin-dentine bond. J Dent 2017;60:77–86.
[55] Mancheno-Posso P, Dittler RF, Lewis D, Juang P, XY JI, Xu XH, et al. Review of status, trends, and challenges in working with silane and functional silanes. In: Moriguchi K, Utagawa S, editors. Silane, chemistry, applications and performance. New York: Nova Science Publishers; 2013. p. 66–87.
[56] Ya-ping G, Ji-yao L, Mohamed MM, Christopher WC, Hockin HKX, Tay FR, et al. Quaternary ammonium silane-based antibacterial and anti-proteolytic cavity cleanser. Dent Mater 2018;12:1814–27.
[57] Baumgartner JC. Microbiologic aspects of endodontic infections. J Calif Dent Assoc 2004;32:459–68.
[58] Stuart CH, Schwartz SA, Beeson TJ, Owatz CB. *Enterococcus faecalis*: its role in root canal treatment failure and current concepts in retreatment. J Endod 2006;32:93–8.
[59] Dumani A, Yoldas O, Yilmaz S, Koksal F, Kayar B, Akcimen B, et al. Polymerase chain reaction of *Enterococcus faecalis* and candida albicans in apical periodontitis from Turkish patients. J Clin Exp Dent 2012;4:e34.
[60] Liu Y, Xu D, Wu Y, Sun H, Gao H. Comparative study on the hydrolysis kinetics of substituted ethoxysilanes by liquid-state 29Si NMR. J Non Cryst Solids 2004;343:61–70.
[61] Inoue N, Tsujimoto A, Takimoto M, Ootsuka E, Endo H, Takamizawa T, et al. Surface free-energy measurements as indicators of the bonding characteristics of single step self-etching adhesives. Eur J Oral Sci 2010;118:525–30.
[62] Daood U, Yiu CKY. Transdentinal cytotoxicity and macrophage phenotype of a novel quaternary ammonium silane cavity disinfectant. Dent Mater 2019;2:206–16.